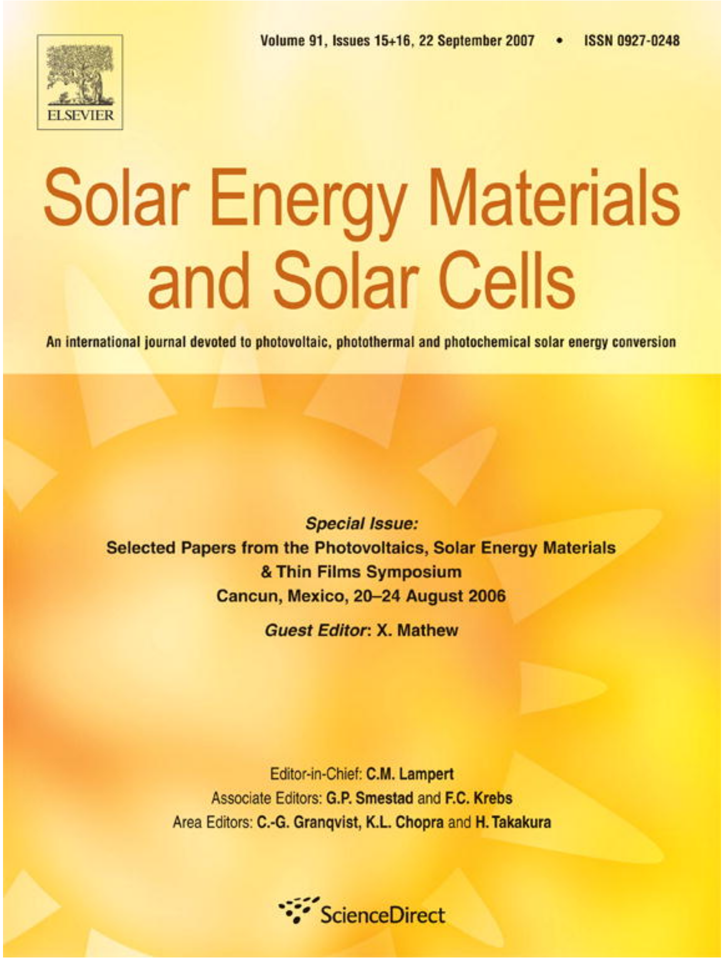

Volume 91, Issues 15+16, 22 September 2007 • ISSN 0927-0248

Solar Energy Materials and Solar Cells

An international journal devoted to photovoltaic, photothermal and photochemical solar energy conversion

Special Issue:
Selected Papers from the Photovoltaics, Solar Energy Materials
& Thin Films Symposium
Cancun, Mexico, 20–24 August 2006

Guest Editor: X. Mathew

Available online at www.sciencedirect.com
ScienceDirect
Solar Energy Materials & Solar Cells 91 (2007) 1458–1461
Solar Energy Materials and Solar Cells
www.elsevier.com/locate/solmat

Electrodeposition of ZnO thin films by using molecular oxygen and hydrogen peroxide as oxygen precursors: Structural and optical properties

D. Ramírez[a], D. Silva[b], H. Gómez[a], G. Riveros[c], R.E. Marotti[b], E.A. Dalchiele[b,*]

[a]Instituto de Química, Facultad de Ciencias, Universidad Católica de Valparaíso, Casilla 4059, Valparaíso, Chile
[b]Instituto de Física, Facultad de Ingeniería, Herrera y Reissig 565, C.C. 30, 11000 Montevideo, Uruguay
[c]Facultad de Ciencias, Universidad de Valparaíso, Avda, Gran Bretaña 1111, Playa Ancha, Valparaíso, Chile

Abstract

Zinc oxide thin films were potentiostatically electrodeposited from a $ZnCl_2 + LiCl$ bath using two different oxygen precursors: molecular oxygen and hydrogen peroxide. X-ray diffraction (XRD) studies confirmed the presence of the ZnO wurtzite structure with marked preferential orientation along the (0 0 2) axis. The optical transmittance shows a clear absorption edge in the ultraviolet (UV) region which corresponds to an energy band gap of 3.41 ± 0.03 eV. As a general rule the higher band gap energies are related to the more transparent films.

Keywords: Thin films; X-ray diffraction; Optical transmittance; Electrochemical deposition

1. Introduction

Zinc oxide is usually an n-type degenerate compound semiconductor with a wurtzite structure having large band gap energy, which is between 3.2 and 3.4 eV at room temperature [1]. Polycrystalline thin films of ZnO have found numerous applications such as transparent conducting films, transparent windows or nanostructured electrode for solar cells, varistors, bulk acoustic wave devices, and blue and ultraviolet (UV) light emitters [2].

Among other methods, ZnO thin films have been prepared by electrochemical deposition [2–5]. The basic reaction leading to ZnO formation is the generation of hydroxide ions at the electrode surface by cathodic reduction of an oxygen precursor [2,6,7]. Three oxygen precursors have been reported in the literature: nitrate ions [4,5], molecular oxygen [8,9], and hydrogen peroxide [10,11]. Some aspects of the electrochemical synthesis of oxide films have been recently reviewed [6,12]. In the present work, LiCl supporting electrolyte was used instead of the commonly KCl [11,13,14] in view of an eventual later study of p-type doping [15,16]. Here, preliminary results of the structural and optical properties of ZnO thin films obtained by using molecular oxygen and hydrogen peroxide oxygen precursors in this media are presented.

2. Experimental

Zinc oxide thin films were grown by potentiostatic electrodeposition from ZnO bath solutions that were prepared by modifying the procedure reported by Pauporté et al. [11], Canava et al. [13] and Yoshida et al. [17]. Briefly, the electrolytic aqueous solution contained $ZnCl_2$ as a zinc precursor, LiCl as a supporting electrolyte, and two different oxygen precursors that have been assayed molecular oxygen and hydrogen peroxide. The electrodeposition was made on translucent substrates consisting of glass plates with a conductive thin film of fluorine-doped tin oxide (SnO_2:F, FTO) on one side, with dimensions of $2 \times 1\,cm^2$ (the effective deposition area was $1\,cm^2$). Prior to the electrodeposition process the substrates were

---

*Corresponding author. Tel.: +598 2 7110905; fax: +598 2 7111630.
E-mail address: dalchiel@fing.edu.uy (E.A. Dalchiele).

0927-0248/$ - see front matter © 2007 Elsevier B.V. All rights reserved.
doi:10.1016/j.solmat.2007.04.017

ultrasonically cleaned in acetone and alcohol for 5 min each one, and then rinsed in water.

A typical three electrode electrochemical cell (150 cm^3) was mounted: the substrate/sample as working electrode, a silver/silver chloride saturated in KCl ($Ag/AgCl_{sat}$) as reference electrode (all potentials given in the text are with respect to this electrode), and a Pt wire as counterelectrode (as in previous work [14]). The electrodepositions were carried out on a potentiostatic way using a computer-controlled Zanher model IM6 potentiostat–galvanostat.

In either case, the electrolytic solution consisted initially in 5 mM $ZnCl_2$ and 0.1 M LiCl. When molecular oxygen precursor was used, O_2 gas was bubbled in the solution until saturation. In the case of hydrogen peroxide precursor, the H_2O_2 was added just before each experiment to achieve the following concentrations: 10, 20 and 40 mM. These last solutions were de-aerated by bubbling argon gas through and over the solution before and during deposition, respectively. Analytical grade reagents were used. All the samples were grown under stirring and at a constant temperature, which eventually was varied from sample to sample from 60 to 80 °C. The applied potential values were selected according to previous voltametric studies (results not shown) and ranged from −0.6 to −1.0 V. For a complete review of these electrochemical studies see the works of Pauporté et al. [11], Canava et al. [13] and Peulon et al. [14]. The synthesis conditions are summarized in Table 1.

The theoretical film thickness (assuming 100% current efficiency) was calculated from the charge exchanged during the deposition experiment by using Faraday law, assuming a two-electron exchange process for each ZnO molecular unit and a density of the deposit close to that of bulk ZnO.

Powder X-ray diffraction (XRD) patterns of the films were recorded with a Philips PW3710 diffractometer using CuK_α radiation. The optical properties of the samples were studied by optical transmittance spectroscopic measurements. The light source was 450 W Xe lamp (ORIEL 6262). Its output was chopped with an SRS SR540 chopper and filtered with an ORIEL 77250 monochromator. After going through the sample the light was detected by an UDT 11-09-001-1 (100 mm^2 wide area UV enhanced unbiased silicon detector), whose response was electronically linearized. Two lock-in amplifiers SRS SR530 and EG&G 5209 extracted the signal from the detector and from a signal reference for noise reduction due to light source fluctuations. A FTO/glass substrate was used as a reference. All measurements were done at room temperature.

3. Results and discussion

Fig. 1 shows typical XRD results for some selected samples, the ones grown at 80 °C for both precursors.

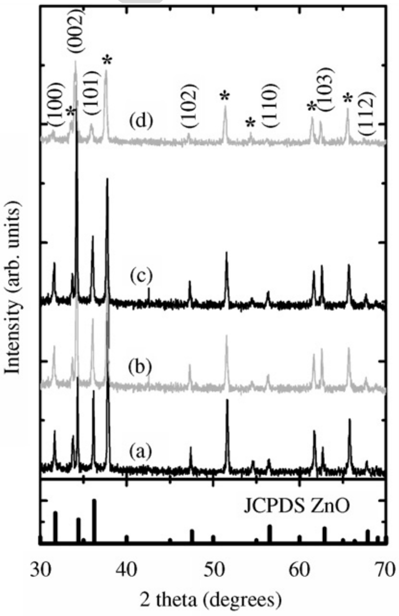

Fig. 1. XRD results for ZnO thin film samples grown at 80 °C: (a) sample ♯2, obtained from 5 mM $ZnCl_2$ + 0.1 M LiCl + O_2 at −0.6 V, thickness: 0.4 μm; (b) sample ♯12, obtained from 5 mM $ZnCl_2$ + 0.1 M LiCl + 10 mM H_2O_2 at −0.9 V, thickness: 1.7 μm; (c) sample ♯13, obtained from 5 mM $ZnCl_2$ + 0.1 M LiCl + 25 mM H_2O_2 at −0.9 V, thickness: 4.0 μm; and (d) sample ♯14, obtained from 5 mM $ZnCl_2$ + 0.1 M LiCl + 40 mM H_2O_2 at −0.9 V, thickness: 1.7 μm.

Table 1
Summary of electrochemical growing conditions of ZnO thin films, thickness and band gap energy (in eV) results

Sample no.	Growing conditions and film thickness						Optical results band gap energy (eV)		
	Zinc precursor	Supporting electrolyte	Oxygen precursor	Bath temperature (°C)	Potential (V)	Film thickness (μm)	dT/dλ E_{peak} (eV)	$(\alpha x h\nu)^2$ vs. hν	$(\alpha x h\nu)^2$ vs. hν (w/o backgr.)
1	5 mM $ZnCl_2$	0.1 M LiCl	sat. O_2	60	−0.6	0.4	3.24	3.24	3.25
2	5 mM $ZnCl_2$	0.1 M LiCl	sat. O_2	80	−0.6	1.3	3.38	3.40	3.41
9	5 mM $ZnCl_2$	0.1 M LiCl	10 mM H_2O_2	60	−0.9	1.3	3.38	3.42	3.42
10	5 mM $ZnCl_2$	0.1 M LiCl	25 mM H_2O_2	60	−0.9	4.0	3.36	3.39	3.40
11	5 mM $ZnCl_2$	0.1 M LiCl	40 mM H_2O_2	60	−0.9	3.6	3.38	3.43	–
12	5 mM $ZnCl_2$	0.1 M LiCl	10 mM H_2O_2	80	−0.9	1.7	3.34	3.39	3.39
13	5 mM $ZnCl_2$	0.1 M LiCl	25 mM H_2O_2	80	−0.9	4.0	3.33	3.36	3.38
14	5 mM $ZnCl_2$	0.1 M LiCl	40 mM H_2O_2	80	−0.9	1.7	3.39	3.44	–

Several peaks are shown, but they can be classified into two groups, the ones marked with an asterisk, which were already present at the substrate; and the one labeled as (1 0 0), (0 0 2), (1 0 1), (1 0 2), (1 1 0), (1 0 3) and (1 1 2), which corresponds to the typical diffraction peaks of hexagonal (wurtzite) ZnO [18]. These results are similar to the ones obtained when KCl supporting electrolyte was used [2,19]. The relative heights between the two groups are due to the different thickness of the electrodeposited films (see Table 1). As a general rule, the diffraction peaks are very narrow, revealing the good crystalline character of the samples. Moreover, the crystallite sizes determined from the peak width by using Scherrer equation were, in general, larger than the accepted uncertainty and resolution value for the method [20]. Furthermore, from Fig. 1, it is clear that the films are preferentially oriented with the (0 0 2) plane parallel to the substrate surface (*c*-axis orientation). In fact, the texture coefficient calculated by the Harris formula, with $N = 9$ [21] is 3.4 for sample 2, grown with molecular O_2 as oxygen precursor, and between 5 and 7 for the ones prepared from H_2O_2. In all these cases, the samples were grown at 80 °C, which is the deposition temperature that gives the highest texture coefficients [22].

The optical properties of the samples were studied by means of optical transmittance. Although the substrate shows a white ("milky") appearance, it has an absorption edge at 327 nm (~3.80 eV). This is a higher value than the expected band gap energy for the ZnO thin films, which is usually reported in the region between 3.1 and 3.4 eV [1,5,15]. Therefore, it can be assumed that FTO is transparent in the region of interest for determining ZnO band gap energy. Fig. 2a shows the transmittance in this region and a typical plot for direct band gap energy determination of sample 2, prepared with molecular oxygen as precursor. The transmittance of the sample is very high (on the order of 80%, which reveals the good quality of the films) on the visible part of the spectra, while it falls to very small values in the UV region. Thus, the films show an abrupt absorption edge between 350 and 400 nm, i.e. close to the expected position of ZnO direct band edge absorption. The eighth to tenth columns of Table 1 show several results for direct band gap energy determined by three methods [23]: first derivative transmittance (T) maximum [5,24], $(\alpha \times h\nu)^2$ vs. photon energy $h\nu$ (where $\alpha \approx -\ln T$ is absorption coefficient) and, same as the latter but subtracting a background for indirect or amorphous absorption [25,26], respectively.

The transmittance spectra for samples that were grown with H_2O_2 instead of O_2 (samples 12–14) are shown in Fig. 2b. The spectra of these samples, including those that are not shown, have an appearance similar to that just described. Band gap energy results are summarized in Table 1. Interesting enough for each method the same relation between the results is kept from sample to sample [23]. It is noteworthy that for samples 11 and 14 the results in the last column of Table 1 (direct band gap energy subtracting the background) are missing. The transmittance of these samples in their transparent region (close to 450 nm) is so high (larger than 95%) that no background due to an indirect edge can be found. Therefore, the results of the previous column should be considered as the same as for this case.

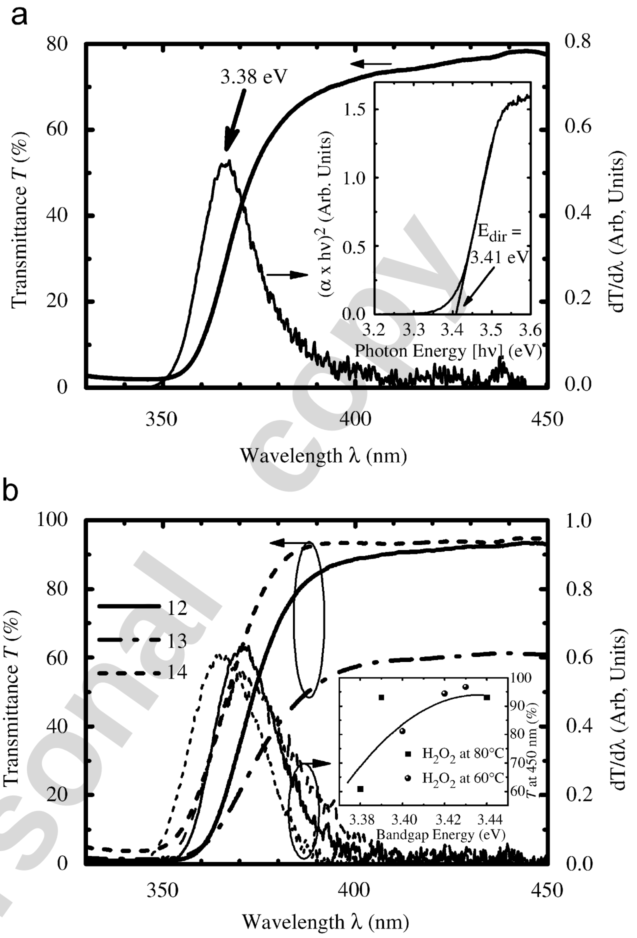

Fig. 2. Transmittance and its first derivate for: (a) sample ♯2, obtained from 5 mM $ZnCl_2$ + 0.1 M LiCl + O_2 at −0.6 V, thickness: 0.4 μm. In inset: plot for finding direct band gap. (b) samples ♯12, ♯13 and ♯14 as indicated, grown with H_2O_2 precursor in solution at 80 °C: sample ♯12, obtained from 5 mM $ZnCl_2$ + 0.1 M LiCl + 10 mM H_2O_2 at −0.9 V, thickness: 1.7 μm; sample ♯13, obtained from 5 mM $ZnCl_2$ + 0.1 M LiCl + 25 mM H_2O_2 at −0.9 V, thickness: 4.0 μm; and sample ♯14, obtained from 5 mM $ZnCl_2$ + 0.1 M LiCl + 40 mM H_2O_2 at −0.9 V, thickness: 1.7 μm. In inset: graph correlating transmittance at 450 nm with band gap energy values. Line is guide for the eyes.

All band gap energy values are quite close to 3.40 eV, i.e. one of the most accepted values for ZnO room temperature band gap energy [1]. The only exception is for sample 1 whose value is lower (3.25 eV), but still within the usually reported region [1]. However, there is no clear tendency of the band gap energy with the deposition parameters. But, as a general rule, the higher band gap energies are related to the more transparent films. This is clearly shown in the inset of Fig. 2b. This indicates that the band gap energy variation may be due to a doping effect [23].

In summary, the previous results confirm that it is possible to grow polycrystalline ZnO thin films with the expected optical properties using LiCl instead of KCl.

4. Conclusions

Zinc oxide thin films were electrodeposited from a $ZnCl_2 + LiCl$ electrolytic bath with two different oxygen precursors, molecular oxygen and hydrogen peroxide. XRD confirmed the presence of the ZnO wurtzite structure with marked preferential orientation along the (0 0 2) axis. Specially for H_2O_2 precursor at 80 °C in which the texture coefficient for this direction is between 5 and 7. The band gap energy was found to be 3.41 ± 0.03 eV. The visible transmittance of the films is typically 80%. For some films which show a milky appearance it falls to 60%, while it increases close to 100% for other films.

Acknowledgments

E.A.D. and R.E.M. acknowledge the support received from PEDECIBA-Física, and the CSIC (Comisión Sectorial de Investigación Científica) of the Universidad de la República, in Montevideo, Uruguay. The present work has been supported by FONDECYT (Project no. 1040650), Chile.

References

[1] R.N. Bhargava (Ed.), Properties of Wide Band Gap II–VI Semiconductors EMIS Datareviews Series No. 17,, INSPEC, London, UK, 1997.
[2] A. Goux, T. Pauporté, J. Chivot, D. Lincot, Electrochim. Acta 50 (2005) 2239.
[3] M. Izaki, T. Omi, J. Electrochem. Soc. 143 (1996) L53.
[4] E.A. Dalchiele, P. Giorgi, R.E. Marotti, F. Martín, J.R. Ramos-Barrado, R. Ayouci, D. Leinen, Sol. Energy Mater. Sol. Cells 70 (2001) 245.
[5] R.E. Marotti, D.N. Guerra, C. Bello, G. Machado, E.A. Dalchiele, Sol. Energy Mater. Sol. Cells 82 (2004) 85.
[6] G.H.A. Therese, P.V. Kamath, Chem. Mater. 12 (2000) 1195.
[7] T. Pauporté, D. Lincot, Electrochim. Acta 45 (2000) 3345.
[8] S. Peulon, D. Lincot, Adv. Mater. 8 (1996) 166.
[9] T. Pauporté, D. Lincot, Appl. Phys. Lett. 75 (1999) 3817.
[10] T. Pauporté, D. Lincot, J. Electrochem. Soc. 148 (2001) C310.
[11] T. Pauporté, D. Lincot, J. Electroanal. Chem. 517 (2001) 54.
[12] Y. Matsumoto, MRS Bull. 12 (2000) 47.
[13] B. Canava, D. Lincot, J. Appl. Electrochem. 30 (2000) 711.
[14] S. Peulon, D. Lincot, J. Electrochem. Soc. 145 (1998) 864.
[15] D.P. Norton, Y.W. Heo, M.P. Ivill, K. Ip, S.J. Pearton, M.F. Chisholm, T. Steiner, Mater. Today (2004) 34.
[16] S.J. Pearton, D.P. Norton, K. Ip, Y.W. Heo, T. Steiner, Prog. Mater. Sci. 50 (2005) 293.
[17] T. Yoshida, T. Pauporté, D. Lincot, T. Oekermann, H. Minoura, J. Electrochem. Soc. 150 (2003) C608.
[18] JCPDS, file 5-0664, ZnO, 1992.
[19] Y. Leprince-Wang, A. Yacoubi-Ouslim, G.Y. Wang, Microelectron. J. 36 (2005) 625.
[20] B.D. Cullity, Elements of X-ray Diffraction, second ed., Addison-Wesley, Reading, MA, 1978.
[21] G.B. Harris, Philos. Mag. 43 (1952) 113.
[22] R.E. Marotti, P. Giorgi, G. Machado, E.A. Dalchiele, Sol. Energy Mater. Sol. Cells 90 (2006) 2356.
[23] C. D. Bojorge, H. R. Cánepa, U. E. Gilabert, D. Silva, E. A. Dalchiele, R. E. Marotti, J. Mater. Sci. Mater. Electron., in press.
[24] G. Riveros, H. Gómez, R. Henríquez, R. Schrebler, R.E. Marotti, E.A. Dalchiele, Boletín de la Sociedad Chilena de Química 47 (2002) 411.
[25] J. Tauc, Mater. Res. Bull. 5 (1970) 721.
[26] K. Keis, A. Roos, Opt. Mater. 20 (2002) 35.